nature neuroscience

Regulation of T-type calcium channels by Rho-associated kinase

Mircea Iftinca[1–3], Jawed Hamid[1–3], Lina Chen[1–3], Diego Varela[1–3], Reza Tadayonnejad[1,2], Christophe Altier[1–3], Ray W Turner[1,2] & Gerald W Zamponi[1–3]

We investigated the regulation of T-type channels by Rho-associated kinase (ROCK). Activation of ROCK via the endogenous ligand lysophosphatidic acid (LPA) reversibly inhibited the peak current amplitudes of rat $Ca_v3.1$ and $Ca_v3.3$ channels without affecting the voltage dependence of activation or inactivation, whereas $Ca_v3.2$ currents showed depolarizing shifts in these parameters. LPA-induced inhibition of $Ca_v3.1$ was dependent on intracellular GTP, and was antagonized by treatment with ROCK and RhoA inhibitors, LPA receptor antagonists or GDPßS. Site-directed mutagenesis of the $Ca_v3.1$ α_1 subunit revealed that the ROCK-mediated effects involve two distinct phosphorylation consensus sites in the domain II-III linker. ROCK activation by LPA reduced native T-type currents in Y79 retinoblastoma and in lateral habenular neurons, and upregulated native $Ca_v3.2$ current in dorsal root ganglion neurons. Our data suggest that ROCK is an important regulator of T-type calcium channels, with potentially far-reaching implications for multiple cell functions modulated by LPA.

Calcium entry via T-type calcium channels regulates a number of physiological functions, including neuronal burst firing, cardiovascular function, pain transmission, cell proliferation, apoptosis, osteogenesis and tumor formation[1–9]. At the molecular level, T-type channels can be encoded by one of three different α_1 subunit genes, $Ca_v3.1$, $Ca_v3.2$ and $Ca_v3.3$, with no ancillary subunits being required to form a functional channel[4,10]. These different T-type channel subtypes support distinct physiological functions, as is evident from knockout mouse studies: knockout of $Ca_v3.1$ protects from certain types of pharmacologically induced seizures[11], whereas knockout of $Ca_v3.2$ results in compromised vascular function and developmental defects[12]. Hence, selective up- or downregulation of different T-type calcium channel isoforms by intracellular messenger pathways is likely to result in distinct physiological consequences.

LPA is a natural phospholipid released by thrombin-activated platelets that has been linked to a number of neurophysiological processes, such as neuronal growth and development[13,14]. LPA activates five different types of G protein–coupled receptors (GPCRs) termed LPA1 through LPA5, of which LPA1 is the major subtype expressed in the adult brain[15–19]. LPA receptors are promiscuous in their coupling to different types of G protein α subunits[17,18]. This includes coupling to $G\alpha_q$ (LPA1–5) to activate phospholipase C and protein kinase C (PKC), $G\alpha_i$ (LPA1–3) to inhibit protein kinase A (PKA), and $G\alpha_s$ (LPA4) to activate PKA. LPA1 (also known as EDG2), LPA2 (also known as EDG4), LPA4 (ref. 20) and LPA5 (ref. 19) also signal via $G\alpha_{12/13}$ to activate RhoA, a member of the family of Rho GTPases. These GTPases show changing levels of expression during the cell cycle and maturation and are important in regulating transcription, neurite outgrowth, myogenesis, cell transformation and tumorgenesis[13,14,21–27]. The first and best characterized effectors of Rho GTPases are the Rho-associated serine/threonine protein kinases[28,29]. There are two known isoforms, ROCK I and ROCK II, both of which are ubiquitously expressed in mouse and rat tissues[23,27,29] and phosphorylate a variety of targets such as potassium and sodium channels[30,31]. Under basal conditions, the C terminus of ROCK serves as an autoinhibitory domain that blocks kinase activity[32]. Binding of GTP-bound RhoA is believed to disrupt this autoinhibition and allow the catalytic domain of ROCK to phosphorylate target proteins[23,33]. Because ROCK and T-type calcium channel activity are linked to overlapping physiological responses, we examined whether ROCK activity might regulate T-type channels.

Here we show that RhoA-induced activation of ROCK inhibits $Ca_v3.1$ T-type calcium channels via phosphorylation of amino acid residues in the domain II-III linker region of the channel. We further show that LPA inhibits native T-type currents in both Y79 retinoblastoma neurons and in lateral habenula (LHb) neurons ($Ca_v3.1$) with a corresponding block of rebound burst discharge, but upregulates $Ca_v3.2$ current in dorsal root ganglion (DRG) neurons.

RESULTS

Inhibition of $Ca_v3.1$ current by LPA

We examined the effect of LPA on rat $Ca_v3.1$ channels that were transiently expressed in tsA-201 cells (**Fig. 1**). Under control conditions, $Ca_v3.1$ channels showed all of the hallmarks of T-type channels, including rapid inactivation kinetics and activation at negative membrane potentials. Exposure of $Ca_v3.1$ expressing cells to 10 μM LPA

[1]Hotchkiss Brain Institute, Departments of Physiology & Biophysics, [2]Cell Biology & Anatomy and [3]Pharmacology & Therapeutics, University of Calgary, 3330 Hospital Drive N.W., Calgary, T2N 4N1, Canada. Correspondence should be addressed to G.W.Z. (zamponi@ucalgary.ca).

Received 27 March; accepted 10 May; published online 10 June 2007; doi:10.1038/nn1921

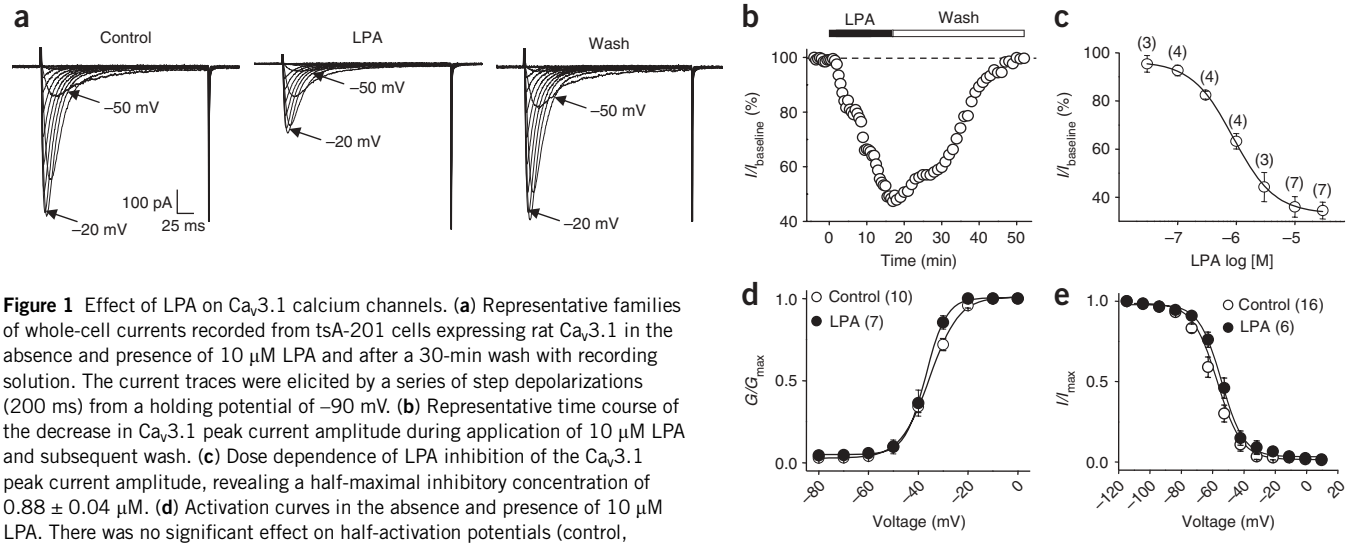

Figure 1 Effect of LPA on $Ca_v3.1$ calcium channels. (**a**) Representative families of whole-cell currents recorded from tsA-201 cells expressing rat $Ca_v3.1$ in the absence and presence of 10 μM LPA and after a 30-min wash with recording solution. The current traces were elicited by a series of step depolarizations (200 ms) from a holding potential of –90 mV. (**b**) Representative time course of the decrease in $Ca_v3.1$ peak current amplitude during application of 10 μM LPA and subsequent wash. (**c**) Dose dependence of LPA inhibition of the $Ca_v3.1$ peak current amplitude, revealing a half-maximal inhibitory concentration of 0.88 ± 0.04 μM. (**d**) Activation curves in the absence and presence of 10 μM LPA. There was no significant effect on half-activation potentials (control, –35.4 ± 1.0 mV; LPA, –37.2 ± 2.0 mV). (**e**) Voltage dependence of inactivation in the absence and presence of 10 μM LPA. The data were fitted with the Boltzmann equation; V_h values did not differ significantly between control and LPA (control, –57.1 ± 2.2 mV; LPA, –51.7 ± 3.5 mV).

resulted in a ~60% decrease in the peak current ($n = 7$, $P = 0.001$) (**Fig. 1a–c**), which was completely abolished after a 30-min wash (**Fig. 1a,b**). By comparison, washing for 30 min in the absence of LPA did not have a significant effect ($n = 7$; data not shown), thus ruling out the possibility that rundown contributed to the observed effects. The LPA-induced inhibition of $Ca_v3.1$ current was dose dependent (**Fig. 1c**) with a half-maximal effect at 0.88 ± 0.04 μM. Exposure to LPA did not affect the voltage dependence of activation or inactivation (**Fig. 1d,e**), nor did it affect the gating kinetics. The reversibility of the effects suggests that LPA-induced decrease in current amplitude is not due to a loss of channels in the plasma membrane, but instead might be due to a reduction in open probability and/or altered single-channel conductance. Similar results were obtained with human $Ca_v3.1$ channels (66.2 ± 4.5% inhibition, $n = 3$, $P = 0.01$). Collectively, these data illustrate a robust and reversible LPA-mediated inhibition of $Ca_v3.1$ T-type channels.

LPA inhibits $Ca_v3.1$ activity via ROCK

RT-PCR analysis indicates that tsA-201 cells express multiple types of LPA receptors (**Supplementary Fig. 1** online). To discern which receptor types and signaling cascades are involved, we conducted a series of pharmacological experiments on transiently expressed $Ca_v3.1$ channels. LPA was ineffective when GTP was omitted from the internal recording solution (3.8 ± 1.6% decrease by LPA, $n = 9$; **Fig. 2a,b**).

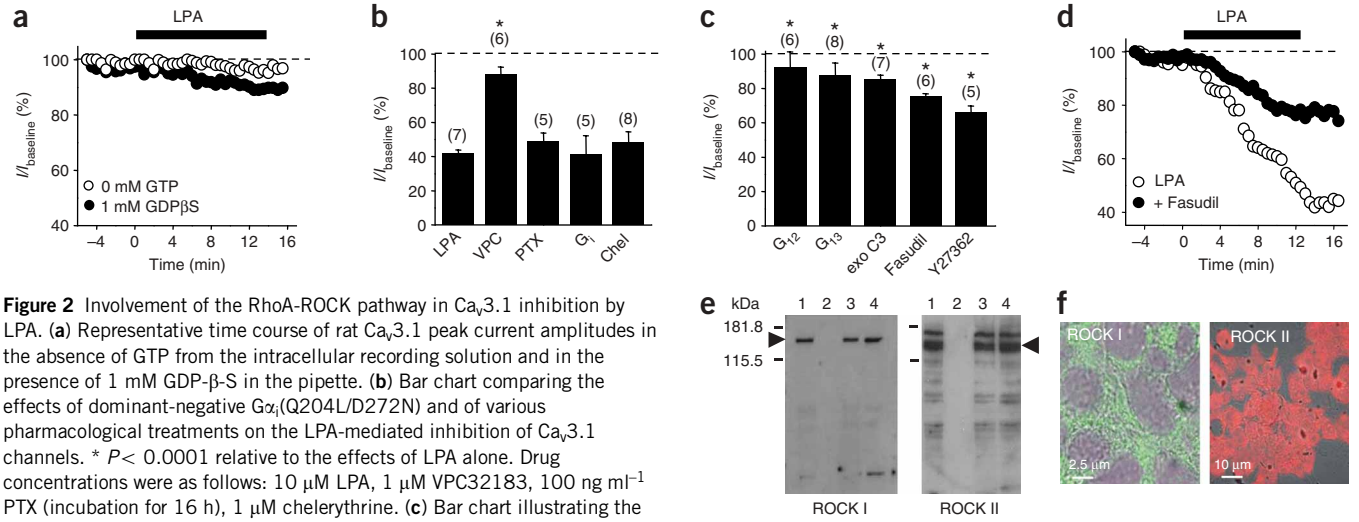

Figure 2 Involvement of the RhoA-ROCK pathway in $Ca_v3.1$ inhibition by LPA. (**a**) Representative time course of rat $Ca_v3.1$ peak current amplitudes in the absence of GTP from the intracellular recording solution and in the presence of 1 mM GDP-β-S in the pipette. (**b**) Bar chart comparing the effects of dominant-negative $G\alpha_i$(Q204L/D272N) and of various pharmacological treatments on the LPA-mediated inhibition of $Ca_v3.1$ channels. * $P < 0.0001$ relative to the effects of LPA alone. Drug concentrations were as follows: 10 μM LPA, 1 μM VPC32183, 100 ng ml^{-1} PTX (incubation for 16 h), 1 μM chelerythrine. (**c**) Bar chart illustrating the effects of dominant-negative $G\alpha_{12}$(Q231L/D299N) and $G\alpha_{13}$(Q226L/D294N) constructs and those of pharmacological treatments designed to disrupt the LPA-RhoA-ROCK pathway. * $0.0023 > P > 0.0001$ relative to the effects of LPA. Drug concentrations were as follows: 4 μg ml^{-1} exoenzyme C3 (incubation for 4–6 h), 10 μM Y27362, 10 μM Fasudil. (**d**) Representative time course of peak current amplitude in response to 10 μM LPA in the absence and presence of 10 μM Fasudil. (**e**) Western blot examining the presence of endogenous ROCK I (left) and ROCK II (right) in tsA-201 cells. Specific immunoreactivity for ROCK I and II was identified in nontransfected cells (lane 1) and in cells transfected with $Ca_v3.1$ (lane 3) or $Ca_v3.1$ and exposed to 10 μM LPA (lane 4). Lane 2 is blank. (**f**) Immunostaining of untransfected cells with ROCK I (left) and ROCK II (right) antibodies. Note that both ROCK isoforms are endogenously expressed.

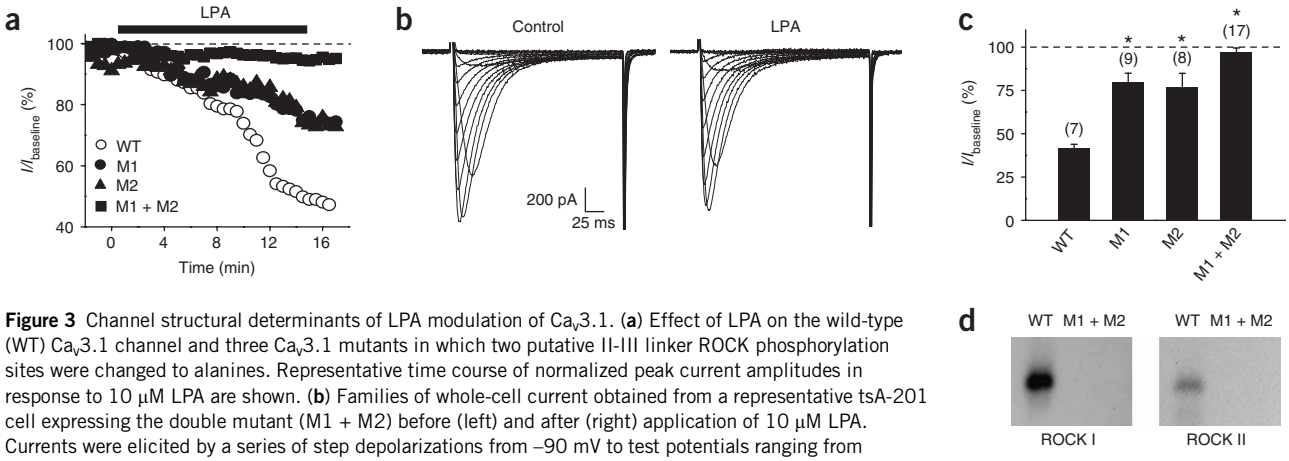

Figure 3 Channel structural determinants of LPA modulation of $Ca_v3.1$. (**a**) Effect of LPA on the wild-type (WT) $Ca_v3.1$ channel and three $Ca_v3.1$ mutants in which two putative II-III linker ROCK phosphorylation sites were changed to alanines. Representative time course of normalized peak current amplitudes in response to 10 μM LPA are shown. (**b**) Families of whole-cell current obtained from a representative tsA-201 cell expressing the double mutant (M1 + M2) before (left) and after (right) application of 10 μM LPA. Currents were elicited by a series of step depolarizations from –90 mV to test potentials ranging from –80 mV to +40 mV. (**c**) Comparison of the inhibitory effects of 10 μM LPA on wild-type and mutant channels. * denote statistical significance ($P < 0.05$) relative to the effect of LPA. (**d**) *In vitro* phosphorylation of II-III linker peptides corresponding to the wild-type or M1 + M2 double mutant $Ca_v3.1$ channel by constitutively active forms of ROCK I and ROCK II. Note that the wild-type peptide is phosphorylated *in vitro* by ROCK I and to a lesser extent by ROCK II, whereas no signal is evident for the mutant peptide.

Similarly, inclusion of GDPβS in the patch pipette prevented the effects of LPA (**Fig. 2a**), which is consistent with the involvement of a G protein. Application of the mixed LPA1/LPA3 receptor antagonist VPC32183 drastically reduced the effects of LPA (**Fig. 2b**), supporting the involvement of an LPA receptor rather than a direct LPA block of T-type channels. Neither the incubation of cells with pertussis toxin (PTX), nor the coexpression of a dominant-negative $G\alpha_i$(Q204L/D272N) construct affected the ability of LPA to inhibit $Ca_v3.1$ channels (**Fig. 2b**), indicating that the effects of LPA are not mediated by a $G\alpha_i$-linked pathway. Similarly, the PKC inhibitor chelerythrine did not affect the LPA-mediated channel inhibition (**Fig. 2b**), suggesting that the $G\alpha_q$-PLC-PKC pathway is not substantially involved. The only LPA receptor subtype known to activate PKA (that is, LPA4) did not appear to be expressed in tsA-201 cells (**Supplementary Fig. 1**), leaving the $G\alpha_{12/13}$-RhoA-ROCK pathway as a possible candidate. Indeed, overexpression of a dominant-negative $G\alpha_{12}$(Q231L/D299N) or $G\alpha_{13}$(Q226L/D294N) construct markedly reduced the effects of LPA (**Fig. 2c**). Furthermore, incubation of cells with exoenzyme C3 (which ADP-ribosylates and thus inactivates RhoA) almost completely inhibited the effects of LPA on $Ca_v3.1$ channels (**Fig. 2c**). Finally, the ROCK inhibitors Y27362 and Fasudil (HA 1077), when applied individually at a concentration of 10 μM, significantly decreased the LPA-mediated inhibition of $Ca_v3.1$ currents (Fasudil, $P < 0.0001$; Y27362, $P = 0.0023$; **Fig. 2c,d**). The combination of Y27362 and Fasudil (22.5 ± 2.3% inhibition, $n = 3$) was not more effective than Fasudil alone ($P > 0.05$). Addition of chelerythrine had only a small additional effect when coapplied with Fasudil (17.1 ± 1.0% inhibition, $n = 3$). None of the above inhibitors substantially affected Cav3.1 currents *per se* (**Supplementary Table 1** online). Western blotting and immunostaining showed that both ROCK isoforms were present in tsA-201 cells irrespective of coexpression of the $Ca_v3.1$ cDNA, and LPA treatment did not appear to affect endogenous ROCK expression (**Fig. 2e,f**). Collectively, these data indicate that an LPA-mediated activation of Rho via LPA receptors leads to ROCK-mediated inhibition of $Ca_v3.1$ channels.

Structural regions contributing to ROCK-mediated inhibition

The consensus amino-acid sequences for ROCK phosphorylation are R/KXS/T or R/KXXS/T (where X is any amino acid)[26,27]. Sequence analysis of the $Ca_v3.1$ channel revealed several possible ROCK-phosphorylation consensus sites that were localized to the N terminus, the domain II-III linker and the carboxy-terminal region (**Supplementary Fig. 2** online). The two consensus motifs located in the II-III linker are highly conserved among all T-type calcium channel isoforms[10]. Because this region appears to be involved in second-messenger regulation of both $Ca_v3.1$ and $Ca_v3.2$ channels by a number of different second-messenger pathways[34–36], we focused on the II-III linker for mutagenesis purposes. The sites were mutated either individually or in combination by replacing clusters of serines/threonines in these sites (Ser^{1031}/Ser^{1032}/Ser^{1033}/Thr^{1034}, termed M1; or Thr^{1044}/Ser^{1045}/Ser^{1046}/Ser^{1047}, termed M2) with alanines. When expressed in tsA-201 cells, the position and shape of the current-voltage relation (**Supplementary Fig. 2**), whole-cell current densities, and voltage dependences of inactivation of the mutant channels were indistinguishable from wild-type $Ca_v3.1$ (data not shown). The response of either one of the mutant $Ca_v3.1$ constructs to LPA was significantly diminished ($P < 0.0001$), although not completely eliminated (**Fig. 3**). In the double mutant, the effects of LPA were virtually abolished (**Fig. 3a–c**). These data indicate that the ROCK-mediated effects on $Ca_v3.1$ current amplitude involve two adjacent ROCK consensus sites in the domain II-III linker of the channel.

To confirm that this site was indeed a direct target for ROCK-mediated phosphorylation, we carried out *in vitro* phosphorylation assays on synthetic $Ca_v3.1$ II-III linker peptides derived from the wild-type or M1 + M2 double mutant sequence. The wild type II-III linker peptide was phosphorylated *in vitro* by a constitutively active ROCK I and to a lesser extent ROCKII, whereas the mutant peptide was not (**Fig. 3d**). These data indicate that ROCK may act directly on the channel.

LPA effects on other types of voltage-gated Ca^{2+} channels

The conservation of the Rho kinase sites on all rat and human Ca_v3 channel isoforms suggests that $Ca_v3.2$ and $Ca_v3.3$ channels may also be subject to LPA/ROCK-mediated regulation. Indeed, application of LPA to $Ca_v3.3$ channels inhibited peak current amplitude similarly to that observed with $Ca_v3.1$ (**Fig. 4a**), without affecting the position or shape of the current-voltage relation (**Fig. 4b**). In contrast, $Ca_v3.2$ channels responded in a more complex manner to LPA. Of the cells tested, 7 out of 15 showed a significant increase in current (19.9 ± 2.3%, $P = 0.0006$), four showed a significant decrease

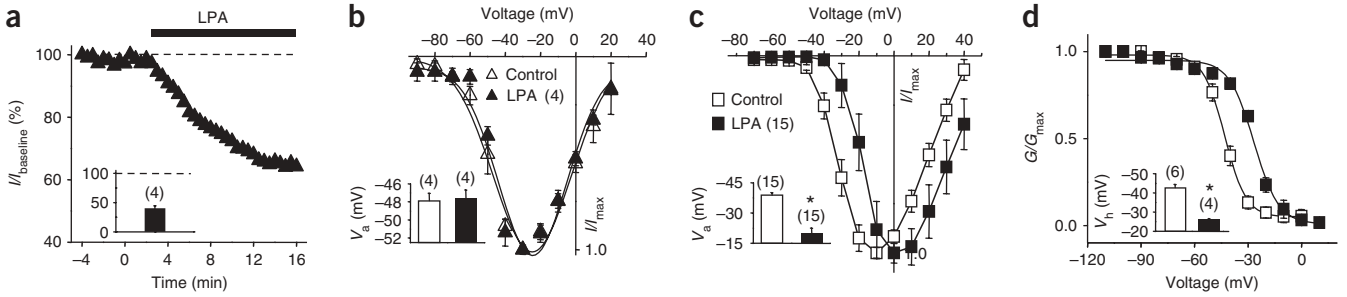

Figure 4 Effect of LPA on $Ca_v3.3$ and $Ca_v3.2$ channel activity. (**a**) Representative time course of the action of LPA on $Ca_v3.3$ channel activity. The percentage of the current remaining after LPA treatment is presented in the inset. As a result of exposure to 10 μM LPA for 15 min the peak current decreased by 60.9 ± 5.5% ($n = 4$). (**b**) Normalized current-voltage relations obtained from $Ca_v3.3$ channels before and after LPA treatment. The half-activation potentials were –48.0 ± 0.9 mV and –47.6 ± 1.0 mV before and after application of 10 μM LPA, respectively ($n = 4$, see inset). (**c**) Normalized current-voltage relations obtained with rat $Ca_v3.2$ channels before and after treatment with 10 μM LPA ($n = 15$). The half-activation potentials were –38.8 ± 1.3 mV and –19.9 ± 2.6 mV ($n = 9$, $P < 0.05$) before and after application of 10 μM LPA, respectively (see inset) . (**d**) Steady state inactivation curves obtained from $Ca_v3.2$ channels before and after treatment with 10 μM LPA. The half-inactivation potentials were –42.8 ± 1.7 and –26.0 ± 0.6 ($n = 6$, $P < 0.05$) before and after application of 10 μM LPA, respectively (see inset). Error bars represent s.e.m.

in current (50.2 ± 9.1%, $P = 0.013$) and four had no significant change ($P = 0.24$). Moreover, unlike the other Ca_v3 channel family members, the voltage dependences of activation and inactivation of $Ca_v3.2$ consistently underwent a 20-mV depolarizing shift on treatment with LPA (**Fig. 4c**,**d**), suggesting a more complex regulation of this channel subtype. LPA also mediated a small, but statistically insignificant ($P = 0.68$), depolarizing shift in reversal potential (control, 43.2 ± 5.5 mV; LPA, 50.7 ± 6.2 mV). It is unclear whether the distinct action of LPA on $Ca_v3.2$ channels is simply due to a different functional response of these channels to ROCK-mediated phosphorylation, or whether the effects may be due to the concerted action of multiple LPA receptor pathways. Nonetheless, the above results indicate that all the T-type channel subtypes are subject to LPA-induced modulation. Moreover, LPA-induced regulation was also observed with $Ca_v2.1$ (P/Q-type) and $Ca_v2.2$ (N-type) channels (**Supplementary Fig. 3** online).

LPA modulates native T-type currents and rebound bursting

To determine whether LPA regulation also occurs with native T-type calcium channels, we conducted electrophysiological recordings from Y79 retinoblastoma cells. These cells express $Ca_v3.1$ and $Ca_v3.2$ calcium channels whose activities can be readily measured via whole-cell patch clamp[37]. LPA application resulted in a markedly reduced whole-cell T-type current activity (**Fig. 5a**), which was prevented by treatment with Fasudil (LPA, 84.2 ± 2.7% inhibition, $n = 6$; LPA+ Fasudil, 18.8 ± 3.1% inhibition, $n = 6$, $P = 0.00006$). The magnitude of the LPA effect appeared to be greater than that observed in transient expression systems, which might be due to the fact that unique $Ca_v3.1$ splice isoforms are present in Y79 cells[2] or that there are regulatory elements specific to these cells. We were unable to hold these cells long enough to directly examine the reversibility of the LPA effects. Instead, intact cells were exposed to 10 μM LPA for 15 min before whole-cell recordings.

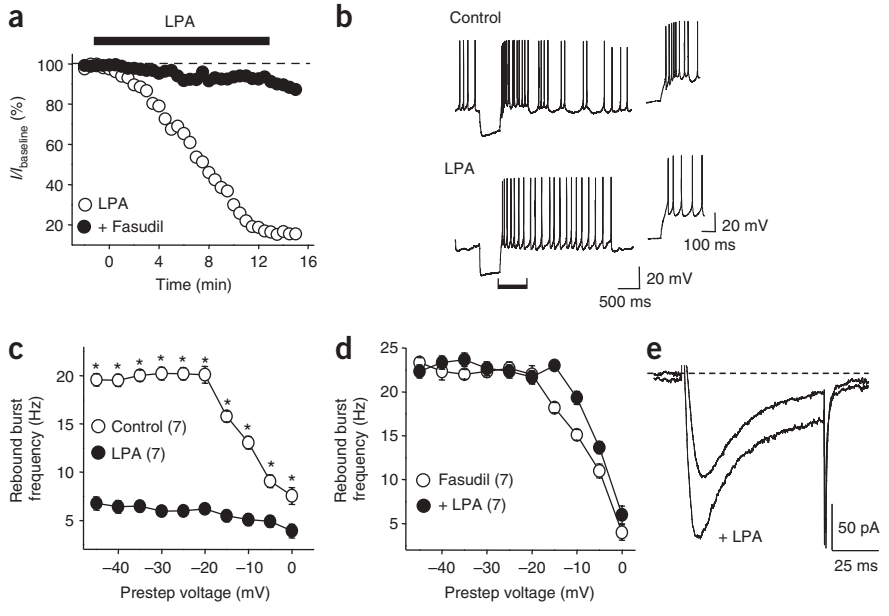

Figure 5 LPA regulation of native T-type currents. (**a**) Representative time courses of peak LVA (T-type) current recorded from Y79 cells in response to 10 μM LPA in the absence and presence of 10 μM Fasudil. (**b**) LPA blocks a $Ca_v3.1$ calcium channel–mediated rebound burst in LHb neurons. A tonic resting discharge of sodium spikes is transformed to a rebound spike burst and oscillatory swings in membrane potential following a hyperpolarizing pulse (500 ms), summarized in **c** as a prestep membrane voltage-frequency plot ($n = 7$). LPA (10 μM) blocks rebound burst discharge without affecting spike threshold. Inset, expansion of the rebound burst phase over the time frame indicated by the horizontal bar below spike traces. (**c**,**d**) Comparison of LPA effects on rebound burst frequency without Fasudil (**c**) or with prior application of Fasudil (**d**). LPA reduces rebound burst frequency. Fasudil (10 μM) application slightly enhanced the oscillatory component of bursting without affecting intraburst spike frequency, and occluded the effects of subsequent LPA application ($n = 7$). * $P < 0.05$ relative to LPA.(**e**) Representative whole-cell recordings of T-type currents obtained from acutely dissociated rat DRG neurons before and after application of 10 μM LPA. The holding potential was –100 mV and the test potential was –40 mV. The external recording solution was supplemented with ω-conotoxin GVIA, agatoxin IVA and nifedipine.

After patch rupture, T-type currents were monitored while LPA was washed off. Under these conditions, T-type current amplitude increased approximately twofold on washout (current densities increased from 4.07 ± 0.7 pA/pF to 8.37 ± 0.9 pA/pF, $n = 11$), indicating that the effects of LPA on T-type current activity in Y79 cells are partially reversible.

We also conducted whole-cell voltage clamp recordings of Ca_v3 current from cells isolated from the rat LHb nucleus in an *in vitro* slice preparation (see Methods). These cells generate prominent rebound bursts that reflect the activation of T-type calcium currents[38,39]. Moreover, we recently determined that LHb cells have among the highest levels of $Ca_v3.1$ immunolabel of any brain region, with virtually no expression of $Ca_v3.2$ or $Ca_v3.3$ (ref. 40). LPA decreased whole-cell T-type current amplitude by 42.8 ± 10.9% ($n = 7$) without affecting the *I-V* relationship (data not shown). Moreover, LPA was significantly less effective in reducing LHb neuron Ca_v3 current in Fasudil-treated slices (12.2 ± 9.3%, $n = 7$, $P = 0.0001$ versus LPA alone). To determine if this reduced T-type calcium channel activity altered the rebound burst firing of LHb neurons, we carried out whole-cell current clamp recordings. Under control conditions, LHb cells showed a tonic spike discharge of 4.6 ± 0.72 Hz ($n = 7$) at approximately –50 mV resting level. Injecting current pulses (500 ms) to evoke hyperpolarizing membrane voltage shifts evoked a transient rebound burst of 5–20 sodium spikes upon return to resting level (20.9 ± 3.03 Hz from –100 mV, $n = 7$; **Fig. 5b**). Spikes evoked during rebound bursts discharged on top of a low voltage–activated (LVA) calcium-dependent depolarization became more evident as the hyperpolarizing prestep was increased[38]. In two of seven cells, the rebound further extended to 2–4 oscillatory swings of LVA responses and associated burst discharge. LPA application (10 μM) tonically depolarized the membrane by ~10 mV (restabilized to control values of –50 mV with bias current injection of approximately –15 pA), but had no significant effect on spike voltage threshold ($n = 7$, $P = 0.69$; **Supplementary Table 2** online). In contrast, the rebound burst and underlying LVA calcium-mediated depolarization was consistently blocked by LPA application, as reflected by a sharp decrease in rebound sodium-spike frequency over the entire range of a voltage-frequency plot ($n = 7$; **Fig. 5c**) and an increase in the prestep voltage threshold (approximately –15 mV) required to generate a LVA response. Both effects were partially reversed after a 15-min wash with artificial cerebrospinal fluid. Exposure to Fasudil slightly lowered the frequency of slow oscillations, but did not substantially increase intraburst spike frequency or spike threshold (**Supplementary Table 2**). Most notably, Fasudil blocked the effects of subsequent LPA application, with little change in the voltage-frequency relationship or threshold for generating a rebound spike burst (**Fig. 5d**). Taken together, our data on LHb neurons suggest that inhibition of T-type current activity via the LPA-ROCK pathway can dramatically regulate neuronal firing frequency and burst output in cells showing prominent $Ca_v3.1$ expression.

Finally, we examined the effects of LPA on native T-type channels in rat DRG neurons expressing robust T-type currents[41] that are carried almost exclusively by $Ca_v3.2$ (ref. 7). Application of LPA to acutely dissociated DRG neurons resulted in a significant increase in T-type current amplitude by 76.7 ± 32.6% ($P < 0.0001$) in five out of six cells, with one additional cell showing a decrease (**Fig. 5e**). Moreover, as with transiently expressed $Ca_v3.2$ channels, a depolarizing shift in half-activation potential was observed (data not shown). After pretreatment of the cells with 10 μM Fasudil, LPA caused a small decrease in current activity (14.0 ± 5.1%, $n = 7$), indicating that inhibition of ROCK activity blocks the LPA-mediated enhancement of native $Ca_v3.2$ channels ($P = 0.008$).

Collectively, these data suggest that native Cav3.1 and Cav3.2 calcium channels can be regulated by activation of the LPA-ROCK pathway.

DISCUSSION

We report here that the activities of both native and transiently expressed T-type calcium channels are regulated via LPA, an endogenous ligand of a class of GPCRs. There are five known types of LPA receptors with varying tissue distributions and developmental expression patterns[17,18]. LPA signaling is complicated because most of these receptors are capable of activating a number of different intracellular messenger pathways by coupling to multiple G protein α subunit subtypes. Our data showing that application of an LPA receptor antagonist, removal of intracellular GTP or intracellular dialysis with GDPβS blocked the LPA-mediated inhibition of $Ca_v3.1$ channels are consistent with LPA receptor–mediated activation of a Gα subunit. Moreover, our data implicate all of the known steps involved in ROCK activation, as the inhibitory effects of LPA were blocked on coexpression of dominant-negative $G\alpha_{12}$ and $G\alpha_{13}$ constructs by elimination of RhoA via exoenzyme C3 and by two pharmacological inhibitors of ROCK. In contrast, PTX, coexpression of dominant-negative $G\alpha_i$, and chelerythrine were ineffective, ruling out contributions by $G\alpha_i$-linked pathways and PKC. Indeed, PKC reportedly upregulates T-type channel activity[36], which is opposite to the observed LPA effects. Finally, elimination of two ROCK consensus sites in the $Ca_v3.1$ domain II-III linker abolished the effects of LPA. Fasudil and Y27362 both act directly on ROCK I and ROCK II[42], and there are no selective inhibitors available that discriminate among the two ROCK isoforms. Our *in vitro* phosphorylation experiments indicated that ROCK I and ROCK II are capable of phosphorylating the channel, although ROCK I appeared to be more effective. Collectively, our data indicate a potent ROCK-dependent inhibition of T-type channel activity that can be triggered by LPA. In tsA-201 cells, the inhibition was prevented by the mixed LPA1 and LPA3 receptor antagonist VPC3218. Given that LPA1, but not LPA3, receptors activate the RhoA-ROCK pathway, we would predict the involvement of LPA1 receptors. Indeed, mRNA encoding LPA1 receptors was detected by RT-PCR, and endogenous expression of LPA1 protein was confirmed by western blotting (data not shown). LPA receptors are part of the family of EDG receptors, which includes receptor subtypes that are activated by sphingosine-1-phosphate (S1P), a lysophospholipid that is structurally related to LPA. At least four of the S1P receptors also couple to the RhoA-ROCK pathway via $G\alpha_{12/13}$[17], and it remains to be determined whether T-type channel activity could also be subject to S1P regulation.

Our data obtained from LHb slices reveal a clear linkage between LPA receptor activation and altered neuronal firing properties. The ability of Fasudil to prevent LPA from decreasing whole-cell T-type current amplitude and rebound bursting is fully consistent with our observations from tsA-201 cells, and suggests that LPA-mediated regulation of burst firing depends on ROCK activation. Nonetheless, we acknowledge the possibility that ROCK may activate additional signaling pathways in neurons that could give rise to a more complex regulation of native T-type currents by LPA. LHb neurons robustly express $Ca_v3.1$ channels[40] and appear to rely on these channels for rebound burst activity following membrane hyperpolarizations. $Ca_v3.1$ knockout mice show reduced burst firing in thalamocortical relay neurons and resistance to baclofen-induced seizures. It will thus be interesting to determine if LPA can protect from pharmacologically induced seizures by reducing T-type channel activity and neuronal firing in the thalamocortical network.

LPA-mediated activation of Rho kinase activity is an important requirement for the development of neuropathic pain at the spinal

level[43]. Conversely, antisense knockdown of spinal $Ca_v3.2$ channels *in vivo* protects against neuropathic pain[7], whereas enhanced $Ca_v3.2$ channel activity in DRG neurons results in peripheral pain sensitization[44]. Our data showing that LPA is capable of increasing the activities of native $Ca_v3.2$ channels in DRG neurons could be consistent with the pronociceptive effects of LPA. However, LPA-ROCK activity is also expected to affect other molecular targets that could contribute to pain sensitization, as LPA is required for injury-induced upregulation of calcium channel α_2-δ subunits[43], with additional LPA receptor expression in Schwann cells[43]. Further work will be required to establish the relative influence of the LPA-induced upregulation of $Ca_v3.2$ channel activity in DRG neurons and pain responses.

There is considerable overlap in the expression patterns of ROCK isoforms and T-type channels not only in neurons, but also in other cell types[4,6,9,22,23,40]. Moreover, there appears to be some commonality in the functional roles of T-type channels and the known functions of the RhoA-ROCK pathway. For example, both ROCK and T-type channels are involved in neuronal outgrowth. Inhibition of ROCK activity or knockdown of Rho promotes axonal regeneration[22,23,45,46], whereas LPA release by neutrophils results in DRG neuronal-process retraction[46]. Similarly, mice lacking $Ca_v3.1$ channels present with bradycardia[8]. Such a phenotype is also observed in transgenic mice overexpressing a constitutively active RhoA mutant[47], which, according to our findings, would be expected to downregulate $Ca_v3.1$ activity. Such putative linkages between Rho activation and T-type channel activity need to be confirmed experimentally, but together provide a compelling case for important interactions between Rho-ROCK activation and T-type channels in numerous physiological processes.

In summary, we have identified a previously unknown pathway for T-type calcium channel regulation by a naturally occurring ligand released at sites known to express both ROCK and T-type calcium channels. The potent inhibition of these channels by ROCK activation suggests that this modulation is important in neuronal physiology.

METHODS

Methodologies for construction of mutant $Ca_v3.1$ channels, data analysis for electrophysiological recordings, and for immunostaining and western blotting for ROCK are described in the **Supplementary Methods** online.

Reagents. Wild-type rat LVA[10] and high voltage–activated calcium-channel subunit cDNA constructs were provided by T. Snutch (University of British Columbia). cDNAs encoding dominant-negative $G\alpha_{12}$(Q231L/D299N; GenBank Accession number L01694), $G\alpha_{13}$(Q226L/D294N; GenBank accession number NM_006572) or $G\alpha_i$(Q204L/D272N; GenBank accession number NM_002069) were obtained from the University of Missouri-Rolla cDNA resource center. The effectiveness of the $G\alpha_i$(Q204L/D272N) construct was verified by its ability to block ORL1 receptor–mediated inhibition of N-type channels (4.6 ± 12% inhibition, $n = 4$; 58 ± 8% inhibition without $G\alpha_i$, $n = 4$). The specificity of the $G\alpha_{13}$(Q226L/D294N) is supported by its inability to block $G\alpha_q$ mediated responses[48]. All drugs were purchased from Sigma with the exception of Y27632 (EMD Biosciences), VPC32183 (Avanti Polar Lipids) and exotoxin C3 (Cytoskeleton). Drugs were dissolved in DMSO at the following stock concentrations: 10 mM LPA, 10 mM Fasudil, 10 mM Y27632 and 1 mM VPC32183. Ca_v3 currents were not affected by 0.1% DMSO. PTX and exoenzyme C3 were prepared in water at a concentration of 1 mg ml^{-1} and 4 mg ml^{-1}, respectively.

Electrophysiological measurements. Tissue culture and transfection of HEK cells were carried out as previously described[49]. Cells were placed into a solution of 5 mM $BaCl_2$, 1 mM $MgCl_2$, 10 mM HEPES, 40 mM TEA-Cl and 87.5 mM CsCl, pH 7.2 adjusted with TEA-OH, and placed on the stage of an epi-fluorescence microscope (Diaphot-TMD, Nikon). HEK cells expressing the transfected $Ca_v3.1$ isoform were identified via enhanced green fluorescent protein fluorescence. Membrane currents were measured using conventional whole-cell patch clamp with pipettes pulled on a Sutter P-87 puller (Sutter Instruments) and polished to 2–4 MΩ resistance with an MF 830 microforge (Narishige). The pipette electrolyte contained: 108 mM $CsCH_3SO_4$, 4 mM $MgCl_2$, 9 mM EGTA, 9 mM HEPES, 1 mM GTP and 5 mM ATP, pH 7.2 adjusted with CsOH. Recordings were carried out using an Axopatch 200B amplifier and pClamp 9.0 software (Axon Instruments). Data were filtered at 1 kHz (8-pole Bessel) and digitized at 10 kHz with a Digidata A/D converter (MDS). Series resistance was 8.6 ± 0.9 MΩ before compensation (~85%), and average cell capacitance was 24.6 ± 1.7 pF. With the exception of experiments in which current densities were compared, typically only currents smaller than 1,200 pA (current density of 42.65 ± 4.87 pA/pF) were used for analysis to reduce voltage errors to <2 mV. Only those cells that showed a stable voltage control throughout the recording were used for analysis.

DRG neurons from neonatal rats were acutely dissociated and plated as described previously[49]. Recordings from DRG neurons were carried out under the experimental conditions reported by us previously[49], with the exception that the external recording solution was supplemented with 500 nM ω-conotoxin GVIA, 300 nM ω-agatoxin IVA and 1 μM nifedipine. Y79 cells were cultured and subjected to whole-cell patch clamp as described previously[37] using the same recording solutions as those for tsA-201 cell recordings (described above). Coronal *in vitro* slices of LHb (400 μm) were prepared from postnatal day 16–21 male Spraque Dawley rats using protocols detailed previously[50]. Slices were maintained on the stage of a Zeiss Axioskop FS-II microscope and recordings were carried out at 32 °C using a Multiclamp 700 amplifier. Artificial cerebrospinal fluid was composed of 125 mM NaCl, 3.25 mM KCl, 1.5 mM $CaCl_2$, 1.5 mM $MgCl_2$, 25 mM $NaHCO_3$ and 25 mM D-glucose. The electrolyte for current-clamp recordings contained: 130 mM potassium gluconate, 0.1 mM EGTA, 10 mM HEPES, 7 mM NaCl, 0.3 mM $MgCl_2$, pH 7.3 with KOH. Bias current was adjusted to maintain a resting value of approximately –50 mV as indicated by the afterhyperpolarization trough. For voltage-clamp recordings, slices were maintained at 21 °C and Ca_v3 current isolated through bath application of 2 mM CsCl, 2 mM TEA and 5 mM 4-AP, with 200 nM TTX, 5 μM nifedipine, 50 μM picrotoxin and 1 mM kynurenic acid to block synaptic activity. The internal solution for voltage-clamp recordings consisted of: 140 mM KCl, 5 mM EGTA, 10 mM HEPES and 2.5 mM $MgCl_2$, pH 7.3 with KOH.

***In vitro* phosphorylation.** The *in vitro* phosphorylation experiments were carried out using two synthetic 40-mer peptides corresponding to $Ca_v3.2$ II-III linker sequences spanning the two putative ROCK consensus sites. Peptides were synthesized, purified by HPLC and characterized by mass spectrometry (University of Calgary peptide synthesis facility). One peptide corresponded to wild-type sequence, the other peptide to that of the M1 + M2 alanine mutant in which both RPCK consensus sites were substituted with alanines. The amino acid sequences of the peptides were as follows: wild type, TAATP MSHP KSSST GVGEA LGSGS RTSSS GSAEP GAAHH; mutant, TAATP MSHPK AAAAG VGEAL GSGSR RAAAA GSAEP GAAHH. All peptides were dissolved in water at 1 mg ml^{-1} and about 6–10 μg were used per assay. *In vitro* phosphorylation assays were carried out using γ^{32}P-ATP (Perkin Elmer, 3000Ci $mmol^{-1}$), constitutively active ROCK-I or constitutively active ROCK-II (Millipore) according to manufacturer's instructions. To confirm the functionality of the purified ROCK isoforms, the ribosomal S6 acceptor peptide (Sigma Catalogue #R9526) and the S6 kinase substrate peptide (Millipore) were used as positive controls. Following the completion of kinase assays, ^{32}P-labeled II-III linker proteins were separated by PAGE and the phosphorylated proteins were detected by exposing the wet gel to Kodak BioMax MS film.

Statistics. All averaged data are plotted as mean ± s.e.m. and statistical significance assessed, unless stated otherwise, using paired or unpaired Student's *t*-test or ANOVA followed by Bonferonni's *post hoc* test with SigmaStat 2.0 software (Access Softek).

Note: Supplementary information is available on the Nature Neuroscience website.

ACKNOWLEDGMENTS

We thank T. Snutch and J. McRory for providing wild-type Ca_v3 cDNAs, and M. Molineux for early recording tests *in vitro*. This work was supported by grants

from the Canadian Institutes for Health Research. R.W.T. and G.W.Z. are Scientists of the Alberta Heritage Foundation for Medical Research (AHFMR). G.W.Z. is a Canada Research Chair. D.V. holds postdoctoral fellowships from the AHFMR and the Heart and Stroke Foundation of Canada.

COMPETING INTERESTS STATEMENT

The authors declare no competing financial interests.

Published online at http://www.nature.com/natureneuroscience
Reprints and permissions information is available online at http://npg.nature.com/reprintsandpermissions

1. Bertolesi, G.E. *et al.* The Ca^{2+} channel antagonists mibefradil and pimozide inhibit cell growth via different cytotoxic mechanisms. *Mol. Pharmacol.* **62**, 210–219 (2002).
2. Latour, I. *et al.* Expression of T-type calcium channel splice variants in human glioma. *Glia* **48**, 112–119 (2004).
3. Panner, A. *et al.* Is there a role for T-type Ca^{2+} channel in glioma cell proliferation? *Cell Calcium* **37**, 105–119 (2005).
4. Perez-Reyes, E. Molecular physiology of low-voltage-activated T-type calcium channels. *Physiol. Rev.* **83**, 117–161 (2003).
5. Rodman, D.M. *et al.* Low-voltage–activated (T-type) calcium channels control proliferation of human pulmonary artery myocytes. *Circ. Res.* **96**, 864–872 (2005).
6. Yunker, A.M. & McEnery, M.W. Immunological characterization of T-type voltage-dependent calcium channel CaV3.1 (α1G) and CaV3.3 (α1I) isoforms reveal differences in their localization, expression and neural development. *J. Bioenerg. Biomembr.* **35**, 533–575 (2003).
7. Bourinet, E. *et al.* Silencing of the Cav3.2 T-type calcium channel gene in sensory neurons demonstrates its major role in nociception. *EMBO J.* **24**, 315–324 (2005).
8. Mangoni, M.E. *et al.* Bradycardia and slowing of the atrioventricular conduction in mice lacking CaV3.1/α1G T-type calcium channels. *Circ. Res.* **98**, 1422–1430 (2006).
9. Gu, Y. *et al.* Osteoblasts derived from load-bearing bones of the rat express both L- and T-like voltage-operated calcium channels and mRNA for α1C, α1D and α1G subunits. *Pflugers Arch.* **438**, 553–560 (1999).
10. McRory, J.E. *et al.* Molecular and functional characterization of a family of rat brain T-type calcium channels. *J. Biol. Chem.* **276**, 3999–4011 (2001).
11. Kim, D. *et al.* Lack of the burst firing of thalamocortical relay neurons and resistance to absence seizures in mice lacking α1G T-type Ca^{2+} channels. *Neuron* **31**, 35–45 (2001).
12. Chen, C.C. *et al.* Abnormal coronary function in mice deficient in α1H T-type Ca^{2+} channels. *Science* **302**, 1416–1418 (2003).
13. Moolenaar, W.H., Kranenburg, O., Postma, F.R. & Zondag, G.C. Lysophosphatidic acid: G protein signalling and cellular responses. *Curr. Opin. Cell Biol.* **9**, 168–173 (1997).
14. Moolenaar, W.H. Development of our current understanding of bioactive lysophospholipids. *Ann. NY Acad. Sci.* **905**, 1–10 (2000).
15. Contos, J.J. & Chun, J. The mouse lp(A3)/Edg7 lysophosphatidic acid receptor gene: genomic structure, chromosomal localization and expression pattern. *Gene* **267**, 243–253 (2001).
16. An, S., Bleu, T., Hallmark, O.G. & Goetzl, E.J. Characterization of a novel subtype of human G protein-coupled receptor for lysophosphatidic acid. *J. Biol. Chem.* **273**, 7906–7910 (1998).
17. Anliker, B. & Chun, J. Cell surface receptors in lysophospholipid signaling. *J. Biol. Chem.* **279**, 20555–20558 (2004).
18. Gardell, S.E., Dubin, A.E. & Chun, J. Emerging medicinal roles for lysophospholipid signaling. *Trends Mol. Med.* **12**, 65–75 (2006).
19. Lee, C-W., Rivera, R., Gardell, S., Dubin, A.E. & Chun, J. GPR92 as a new G12/13- and Gq-coupled lysophosphatidic acid receptor that increases cAMP, LPA5. *J. Biol. Chem.* **281**, 23589–23597 (2006).
20. Yanagida, K., Ishii, S., Hamano, F., Nogichi, K. & Shimizu, T. LPA4/p2y9/GPR23 mediates rho-dependent morphological changes in a rat neuronal cell line. *J. Biol. Chem.* **282**, 5814–5824 (2007).
21. Aznar, S. & Lacal, J.C. Rho signals to cell growth and apoptosis. *Cancer Lett.* **165**, 1–10 (2001).
22. Mueller, B.K., Mack, H. & Teusch, N. Rho kinase, a promising drug target for neurological disorders. *Nat. Rev. Drug Discov.* **4**, 387–398 (2005).
23. Riento, K. & Ridley, A.J. Rocks: multifunctional kinases in cell behaviour. *Nat. Rev. Mol. Cell Biol.* **4**, 446–456 (2003).
24. Shimokawa, H. & Takeshita, A. Rho-kinase is an important therapeutic target in cardiovascular medicine. *Arterioscler. Thromb. Vasc. Biol.* **25**, 1767–1775 (2005).
25. Dergham, P. *et al.* Rho signaling pathway targeted to promote spinal cord repair. *J. Neurosci.* **22**, 6570–6577 (2002).
26. Kawano, Y. *et al.* Phosphorylation of myosin-binding subunit (MBS) of myosin phosphatase by Rho-kinase *in vivo*. *J. Cell Biol.* **147**, 1023–1038 (1999).
27. Nakagawa, O. *et al.* ROCK-I and ROCK-II, two isoforms of Rho-associated coiled-coil forming protein serine/threonine kinase in mice. *FEBS Lett.* **392**, 189–193 (1996).
28. Matsui, T. *et al.* Rho-associated kinase, a novel serine/threonine kinase, as a putative target for small GTP binding protein Rho. *EMBO J.* **15**, 2208–2216 (1996).
29. Leung, T., Manser, E., Tan, L. & Lim, L. A novel serine/threonine kinase binding the Ras-related RhoA GTPase which translocates the kinase to peripheral membranes. *J. Biol. Chem.* **270**, 29051–29054 (1995).
30. Storey, N.M., O'Bryan, J.P. & Armstrong, D.L. Rac and Rho mediate opposing hormonal regulation of the ether-a-go-go-related potassium channel. *Curr. Biol.* **12**, 27–33 (2002).
31. Staruschenko, A. *et al.* Rho small GTPases activate the epithelial Na^{+} channel. *J. Biol. Chem.* **279**, 49989–49994 (2004).
32. Amano, M. *et al.* The COOH terminus of Rho-kinase negatively regulates rho-kinase activity. *J. Biol. Chem.* **274**, 32418–32424 (1999).
33. Shimizu, T. *et al.* Parallel coiled-coil association of the RhoA-binding domain in Rho-kinase. *J. Biol. Chem.* **278**, 46046–46051 (2003).
34. Wolfe, J.T., Wang, H., Howard, J., Garrison, J.C. & Barrett, P.Q. T-type calcium channel regulation by specific G-protein $\beta\gamma$ subunits. *Nature* **424**, 209–213 (2003).
35. Welsby, P.J. *et al.* A mechanism for the direct regulation of T-type calcium channels by Ca^{2+}/calmodulin-dependent kinase II. *J. Neurosci.* **23**, 10116–10121 (2003).
36. Park, J.Y. *et al.* Activation of protein kinase C augments T-type Ca^{2+} channel activity without changing channel surface density. *J. Physiol. (Lond.)* **577**, 513–523 (2006).
37. Hirooka, K. *et al.* T-Type calcium channel α1G and α1H subunits in human retinoblastoma cells and their loss after differentiation. *J. Neurophysiol.* **88**, 196–205 (2002).
38. Wilcox, K.S., Gutnick, M.J. & Christoph, G.R. Electrophysiological properties of neurons in the lateral habenula nucleus: an *in vitro* study. *J. Neurophysiol.* **59**, 212–225 (1988).
39. Huguenard, J.R., Gutnick, M.J. & Prince, D.A. Transient Ca^{2+} currents in neurons isolated from rat lateral habenula. *J. Neurophysiol.* **70**, 158–166 (1993).
40. McKay, B.E. *et al.* Ca(v)3 T-type calcium channel isoforms differentially distribute to somatic and dendritic compartments in rat central neurons. *Eur. J. Neurosci.* **24**, 2581–2594 (2006).
41. Todorovic, S.M., Jevtovic-Todorovic, V., Mennerick, S., Perez-Reyes, E. & Zorumski, C.F. Ca(v)3.2 channel is a molecular substrate for inhibition of T-type calcium currents in rat sensory neurons by nitrous oxide. *Mol. Pharmacol.* **60**, 603–610 (2001).
42. Davies, S.P., Reddy, H., Caivano, M. & Cohen, P. Specificity and mechanism of action of some commonly used protein kinase inhibitors. *Biochem. J.* **351**, 95–105 (2000).
43. Inoue, M. *et al.* Initiation of neuropathic pain requires lysophosphatidic acid receptor signaling. *Nat. Med.* **10**, 712–718 (2004).
44. Nelson, M.T., Joksovic, P.M., Perez-Reyes, E. & Todorovic, S.M. The endogenous redox agent L-cysteine induces T-type Ca^{2+} channel–dependent sensitization of a novel subpopulation of rat peripheral nociceptors. *J. Neurosci.* **25**, 8766–8775 (2005).
45. Ahmed, Z. *et al.* Disinhibition of neurotrophin-induced dorsal root ganglion cell neurite outgrowth on CNS myelin by siRNA-mediated knockdown of NgR, p75NTR and Rho-A. *Mol. Cell. Neurosci.* **28**, 509–523 (2005).
46. Arimura, N. *et al.* Phosphorylation of collapsin response mediator protein-2 by Rho-kinase. Evidence for two separate signaling pathways for growth cone collapse. *J. Biol. Chem.* **275**, 23973–23980 (2000).
47. Sah, V.P. *et al.* Cardiac-specific overexpression of RhoA results in sinus and atrioventricular nodal dysfunction and contractile failure. *J. Clin. Invest.* **103**, 1627–1634 (1999).
48. Hirdes, W., Horowitz, L.F. & Hille, B. Muscarinic modulation of erg potassium current. *J. Physiol. (Lond.)* **559**, 67–84 (2004).
49. Altier, C. *et al.* Opioid, cheating on its receptors, exacerbates pain. *Nat. Neurosci.* **9**, 31–40 (2006).
50. Molineux, M.L. *et al.* Specific T-type calcium channel isoforms are associated with distinct burst phenotypes in deep cerebellar nuclear neurons. *Proc. Natl. Acad. Sci. USA* **103**, 5555–5560 (2006).